Published in final edited form as:
Clin Neurophysiol. 2012 January ; 123(1): 206–210. doi:10.1016/j.clinph.2011.06.002.

Alteration in surface muscle electrical anisotropy in the rat SOD1 model of amyotrophic lateral sclerosis

Jia Li, PhD and **Seward B. Rutkove, MD**
Beth Israel Deaconess Medical Center, Harvard Medical School, Boston, MA 02215

Abstract

Objective—To evaluate the effects of progressive neurogenic change on surface-measured anisotropy via study in the rat superoxide dismutase 1 (SOD1) G93A amyotrophic lateral sclerosis (ALS) model.

Methods—Eight male ALS rats were studied over a period of 10 weeks. In each, the 20 kHz to 1 MHz electrical impedance of the gastrocnemius-soleus complex was measured with electrodes placed at 0° and at 90° relative to the major muscle fiber direction. The major outcome measure, the anisotropy difference (AD) for each of the resistance, reactance, and phase, was calculated as 90° – 0° values.

Results—All three parameters showed substantial alterations with disease progression. However, the phase AD demonstrated the most substantial change, increasing from 1.8 ± 1.58° to 10.2 ± 2.13° (mean ± standard error) comparing the first and last set of measurements ($p = 0.028$).

Conclusions—Anisotropy increases substantially with disease progression in the ALS rat.

Significance—Measurement of surface electrical anisotropy offers a non-invasive means for quantifying neurogenic change in muscle.

Keywords

Muscle; electrical impedance; amyotrophic lateral sclerosis; anisotropy; rat SOD1 model

1 Introduction

Electrical impedance myography (EIM) is a technique for the evaluation of muscle in which high-frequency, low-intensity electrical current is applied via surface electrodes overlying a muscle of interest and consequent surface voltages measured (Rutkove, 2009). From these voltages, several parameters describing the electrical properties of the muscle can be obtained, including the reactance (X), the resistance (R) and the phase (θ). X represents the time delay between the applied current and the measured voltage, an indication of the muscle's ability to briefly store and release charge; R is the ratio of the applied current to the measured voltage and is an indication of the muscle's ability to transmit an electrical

Correspondence should be addressed to: Seward B. Rutkove, MD, Department of Neurology, Beth Israel Deaconess Medical Center, Boston, MA 02215; Telephone: 617-667-8130; Fax: 617-667-3175 srutkove@bidmc.harvard.edu.

Conflict of interests: Jia Li has no conflicts to report. Seward Rutkove holds equity interest and obtains consulting fees from Convergence Medical Devices, Inc and has 2 patent applications in the field of electrical impedance.

current; θ is a single measure that captures both the X and R and is defined by the trigonometric relation θ = arctan(X / R) (Rutkove et al., 2002). Previous and ongoing work has demonstrated the potential value of EIM in assessing neuromuscular disease states, including in quantifying disease status over time (Rutkove et al., 2007) and also possibly assisting with disease categorization (Garmirian et al., 2009; Rutkove et al., 2010).

One aspect of EIM that to date has received limited attention is that of electrical anisotropy. Electrical anisotropy refers to the presence of a directional-dependence to the measurements. Most body tissues do not demonstrate such dependence and are termed isotropic. Muscle, however, exhibits a strong anisotropy, due to the fact that myocytes are long, tubular structures (Epstein and Foster, 1983; Aaron et al., 1997). Applied electrical current can travel via extra- and intra-cellular paths more easily along muscle fibers than across them. There is also a strong frequency-dependence to this property. In fact, this characteristic of muscle was recognized nearly 50 years ago (Rush 1962; Fatt 1964), but its potential value for muscle disease assessment has only recently been appreciated (Garmirian et al., 2009; Chin et al., 2008).

Recent human studies have suggested that alterations in electrical anisotropy can be observed in both neurogenic and myopathic disease (Garmirian et al., 2009). In myopathy, normally anisotropic muscle fibers are replaced by structures that are relatively isotropic, including inflammatory cells, fat, and connective tissue; thus, the measured anisotropy would be expected to decrease. In neurogenic disease, in contrast, the expectation is less obvious. Progressive neurogenic atrophy could potentially actually enhance anisotropy both through larger structural changes in the muscle and also though elevations in intracellular free water—having the effect of preferentially increasing longitudinal conductivity (Ahad et al., 2010). Changes to the gross shape of the muscle will also influence the anisotropy, regardless of the disease mechanism.

The two previous studies assessing surface anisotropy have been performed in human subjects. In order to study this phenomenon in a more detailed and controlled way, here we describe changes in the surface-measured anisotropy in the SOD1 G93A ALS rat over time with disease progression.

2 Methods

2.1 Animals

All animal work was approved by the Institutional Animal Care and Use Committee of the Beth Israel Deaconess Medical Center, Boston, MA. Eight male SOD1 G93A ALS rats at 8-weeks of age and were obtained from Taconic Laboratories (Germantown, NY). An additional 10 normal animals were obtained from Charles River (Boston, MA) for purposes of assessing the technique’s reproducibility. All of animals were acclimated for 48 hrs after arrival at our animal facility before any testing was initiated.

2.2 Animal setup and EIM

Rats were placed under isoflurane anesthesia in a prone position with the left hind leg extended at approximately a 45° angle away from its body, as previously described (Ahad and Rutkove, 2009). A heating pad was placed underneath the animal to maintain the body temperature at approximately 37° C. The fur overlying the gastrocnemius muscle was removed using a depilatory agent. A pinpoint tattoo was then placed over the approximate midpoint of the muscle to assist in repeat placement of electrodes.

Two 20 mm (L) × 1 mm (W) stainless steel strips were used for current injection whereas two 10 mm (L) × 1 mm (W) served as voltage electrodes. The four strips were placed in a

line onto the adhesive surface of medical adhesive tape (3 M Micropore, 3 M Health Care, St. Paul, Minnesota) with an inter-electrode separation distance of 2 mm. The tetrapolar electrode array was placed both parallel (0°) and perpendicularly (90°) to the major muscle fiber direction to assess the anisotropy (Figure 1).

EIM was performed using a lock-in amplifier, Signal Recovery Model 7280, Advanced Measurement Technology Inc., Oak Ridge TN coupled with a very low capacitance active probe (Model 1103 of Tektronix, Beaverton, OR) as previously described (Esper et al., 2006). Measurements were performed over a frequency range of 20 kHz to 1MHz every other week for 10 weeks, for a total of 6 measurements.

2.3 Motor unit number estimation

MUNE was completed using a TECA Synergy T2 EMG Monitoring System (Viasys, Madison, WI). MUNE was performed on the left hind leg in a position identical to EIM by stimulating the sciatic nerve at the sciatic notch (Neuroline #746 12-100/25 needle electrodes, Ambu, Denmark) and recording via disposable ring electrodes (Product # 019-435500, Faith Medical Inc., Steedman, MO) around the entire leg, similar to how it is performed in the mouse (Shefner et al., 2002). MUNE was performed using the standard incremental method.

2.4 Reproducibility

Immediate reproducibility measurements were performed to evaluate the EIM technique. After the 1st set of measurements was completed, the animal was removed from the measuring area and then placed back. The impedance measurements were then repeated. Although immediate repeatability was not performed for MUNE, reproducibility of the technique was performed by comparing the first week's data set to the second, at a time well before the animals became symptomatic

2.5 Data analysis

Raw resistance and reactance data were collected across the frequency spectrum and phase was calculated. Both longitudinal (0°) and transverse (90°) configuration data were first analyzed separately. The anisotropy difference (AD) was defined as the X, R, or θ value at 90° minus the value obtained at 0°. All results were plotted for the whole frequency spectrum (± standard error); occasional single-frequency outlying data points were deleted based on Chauvenet's criterion.

In addition, the impedance data at 5 single frequencies (50 kHz, 100 kHz, 200 kHz, 300 kHz, and 500 kHz) were used for statistical analyses. Given the small number of animals, non-parametric tests (Wilcoxon rank and Spearman rank tests) were utilized as appropriate. Significance was defined as $p < 0.05$, two-tailed. In the analysis that follows, we first compare just two sets of the data: the initial set of measurements (early stage) performed at a mean of 74 days of age and a final set measurements (late stage) performed 10 weeks later at a mean of approximately 144 days in order to demonstrate the changes in greater relief. We then proceed to review the intervening data points in search of longitudinal trends. For both EIM and MUNE, reproducibility was assessed by calculating intra-class correlation coefficients (ICCs).

3 Results

The immediate reproducibility studies for EIM gave ICCs of 0.92 at 0° and 0.84 at 90° for reactance, 0.68 at 0°. and 0.70 at 90° for resistance, and 0.84 at 0° and 0.88 at 90° for phase.

The week-to-week repeatability was fairly good for MUNE with an ICC of 0.64, comparable to that obtained by other researchers in animals (David et al, 2010).

The alteration in 0° and 90° measurements between early- and late- stage diseased animals is shown in Figure 2. As can be seen, the major alteration with disease is a reduction in the 0° reactance and consequently also in the calculated phase. Resistance values drop slightly at both 0° and 90°. These results for the five frequencies are summarized in Table 1. The changes from early-stage to late-stage of reactance and phase at 0° are significant whereas those for resistance are not. For example, at 100 kHz, reactance at 0° decreased from 17.8 ± 1.17 to 10.9 ± 2.48 ($p = 0.038$) while phase at 0° decreased from 17.4 ± 0.88° to 9.5 ± 1.78° ($p = 0.001$). The corresponding mean MUNE values between these two time points (early-stage vs. late-stage) were 160.6 ± 15.9 to 88.6 ± 19.6.

The AD for the early- and late- stage animals, obtained by subtracting the 0° from the 90° values at each of the 5 frequencies, is shown in Table 2. The statistical analyses show that the anisotropy is increasing (becoming more extreme) for all three measures with disease progression, albeit in the negative direction for resistance. Changes in the AD for reactance and phase,, for example at 100 kHz are significant or near-significant but not for resistance. AD for reactance changed from 1.1 ± 1.86 to 5.6 ± 1.47 ($p = 0.050$) and the AD for phase changed from 1.8 ± 1.58° to 10.2 ± 2.13° ($p = 0.028$). This data confirms that the major change observed is a gradual reduction in the reactance and consequently the phase at 0° as compared to 90°, thus increasing the AD as the disease progresses.

Figure 3 shows the multi-week trends for all the data at both 0° and 90° across the entire set of measurements confirming the gradual reduction in 0° reactance and phase values and relative stability of the resistance values over the time period. Specifically, the longitudinal reactance decreased about 1 Ω per week on average; phase similarly decreased by about 1° per week with disease progression. The correlations to both age and MUNE further indicate that the anisotropy alterations with disease progression were mainly caused by the changes in 0°. The longitudinal reactance and phase values were also significantly correlated to age, whereas resistance values did not. The correlation coefficients are summarized in Table 3.

4 Discussion

The results of this study confirm the increasing anisotropy in all 3 impedance parameters, the resistance, reactance, and phase, with ALS disease progression. These data support our previous limited findings in human subjects, which also demonstrated what appeared to be elevated anisotropy in muscles of patients with ALS (Garmirian et al., 2009). The alteration in the anisotropy difference for phase and reactance appears to be mainly due to a reduction in those values in the longitudinal (0°) direction and little to no change in the transverse (90°). The gradual change over time helps confirm that this alteration in anisotropy is a consistent finding of progressive neurogenic disease.

The mechanism of this change is not clear. One possibility is that alterations in the muscle's inherent electrical properties, its conductivity and permittivity, could be contributing. In fact, a previous study in sciatic crush has shown a substantial elevation in electrical conductivity in the longitudinal direction and much less so in the transverse, thus increasing the actual inherent electrical anisotropy of the muscle (Ahad et al., 2010).

Another possibility is that it simply reflects gross morphological changes in the muscle. As atrophy progresses, the muscle becomes less and less bulbous, gradually transforming into a more cylindrical structure. This alteration in shape could provide a sufficient reason for the change in anisotropy due to the fact that electrical current will not fan out when applied across muscle with a reduced volume (since the reactance is mostly produced by electrical

current crossing myocyte membranes). However, one strong argument against a simple shape effect is the absence of a meaningful change in the resistance anisotropy; indeed if it were simply an effect of the muscle changing shape, even more dramatic alterations in the resistance would be anticipated, however this was not observed.

One approach for determining the influence of shape on these results would be by performing studies in other animal models, such as disuse atrophy and primary muscle disease; such studies are currently under way. Correlating microscopic pathologic changes to the observed impedance data will also help answer this question. An alternative approach would be to perform computer modeling using the finite element method (Wang et al, 2011). We have already initiated this line of research and early data there suggest that changes in shape likely only modestly influence EIM results [unpublished results]. However, a full treatment of this question is still being pursued.

Other factors that could influence these results include variations in temperature and subcutaneous fat thickness. We carefully controlled for the former using a heating pad, maintaining body temperature at close to 37°C throughout the study. Although subcutaneous fat thickness could alter the data, rat subcutaneous fat is extremely thin, and it is therefore unlikely to have a major impact on the anisotropy data. However, the relationship between subcutaneous fat thickness and anisotropy in humans does demand further study and is also being investigated via the finite element method as described above.

The characteristic alterations across the frequency spectrum were also of interest. Frequency-dependence to the changes was observed in our one other study assessing anisotropy alterations in the tibialis anterior muscle of human subjects (Chin et al., 2008), although drawing comparisons between these two investigations is difficult since in that study only two ALS individuals were studied. Interestingly, in that study, the subject with very longstanding atrophy and weakness of the tibialis anterior (the one muscle studied) showed a flattening of the spectrum and reduction in anisotropy, whereas the one with only moderate weakness of the tibialis anterior muscle showed an elevation across the frequency spectrum, suggesting that the duration of neurogenic injury also affects the muscle's anisotropy.

Although relatively good repeatability was achieved with our technique, the methodology itself has a variety of limitations, including the fact that electrodes were far from ideal their being cut from a thin stainless steel sheet. Previous work (Ahad and Rutkove, 2009; Ahad et al., 2009) used larger adhesive electrodes, but that was not possible here given the very small size of the electrodes needed to maintain constant inter-electrode distances at both 0° and 90°. Much of the noise in the measurements is likely due to poor contact between the skin and the metal electrodes. In addition, despite the use of a tattoo, it was impossible to be certain that the electrodes were accurately placed in the identical position and at exactly the same angles across measurement sessions. Atrophy of the underlying muscle would also likely impact the measurements as well, since the electrodes cannot be definitively placed over the exact same region of muscle if it is gradually shrinking. The mean values of MUNE from the initial to the final measurements dropped substantially, from a mean of 161 to 88.6 indicating that the disease is progressing substantially in the 10-week period. Ideally, we would have followed these animals even longer; however, the muscle became so atrophied beyond that point, that it no longer became possible to fit the entire electrode array across the muscle.

In summary, these data confirm the presence of substantial alterations in the anisotropic signature of muscle in ALS and that this change is mostly due to a reduction in longitudinal impedance values in conjunction with a relative stability of the transverse values. This data

confirms and extends the initial observations we have completed in human subjects. Future work to be completed will include studying the anisotropic characteristics of myopathic disease and disuse models to determine if this elevation in anisotropy is observed in all conditions associated with muscle atrophy or if this is a feature uniquely associated with neurogenic disorders.

Acknowledgments

This study was funded by Grant R01NS055099 from the National Institutes of Health.

References

Aaron R, Huang M, Shiffman CA. Anisotropy of human muscle via non-invasive impedance measurements. Phys Med Biol. 1997; 42:1245–62. [PubMed: 9253037]

Ahad MA, Fogerson PM, Rosen GD, Narayanswami P, Rutkove SB. Electrical characteristics of rat skeletal muscle in immaturity, adulthood, and after sciatic nerve injury and their relation to muscle fiber size. Physiol Meas. 2009; 30:1415–27. [PubMed: 19887721]

Ahad MA, Rutkove SB. Electrical impedance myography at 50 kHz in the rat: technique, reproducibility, and the effects of sciatic injury and recovery. Clin Neurophysiol. 2009; 120:1534–8. [PubMed: 19570710]

Ahad MA, Narayanaswami P, Kasselman LJ, Rutkove SB. The effect of subacute denervation on the electrical anisotropy of skeletal muscle: implications for clinical diagnostic testing. Clin Neurophysiol. 2010; 121:882–6. [PubMed: 20153247]

Chin AB, Garmirian LP, Nie R, Rutkove SB. Optimizing measurement of the electrical anisotropy of muscle. Muscle Nerve. 2008; 37:560–5. [PubMed: 18404614]

David WS, Goyal N, Henry FP, Baldassari LE, Redmond RW. Validation of an incremental motor unit number estimation technique in rabbits. Muscle Nerve. 2010 Jun.41:794–9. [PubMed: 20169589]

Epstein BR, Foster KR. Anisotropy in the dielectric properties of skeletal muscle. Med Biol Eng Comput. 1983; 21:51–5. [PubMed: 6865513]

Esper GJ, Shiffman CA, Aaron R, Lee K, Rutkove SB. Assessing neuromuscular disease with multifrequency electrical impedance myography. Muscle Nerve. 2006; 34:595–602. [PubMed: 16881067]

Fatt P. An analysis of the transverse electrical impedance of striated muscle. Proc R Soc Lond B Biol Sci. 1964; 159:606–51. [PubMed: 14130855]

Garmirian LP, Chin AB, Rutkove SB. Discriminating neurogenic from myopathic disease via measurement of muscle anisotropy. Muscle Nerve. 2009; 39:16–24. [PubMed: 19058193]

Rush S. Methods of measuring the resistivities of anisotropic conducting media. J Res NBS. 1962; 66C:217–22.

Rutkove SB. Electrical Impedance Myography: Background, Current State, and Future Directions. Muscle Nerve. 2009; 40:936–46. [PubMed: 19768754]

Rutkove SB, Aaron R, Shiffman CA. Localized bioimpedance analysis in the evaluation of neuromuscular disease. Muscle Nerve. 2002; 35:390–7. [PubMed: 11870716]

Rutkove SB, Shefner JM, Gregas M, Butler H, Caracciolo J, Lin C, et al. Characterizing spinal muscular atrophy with electrical impedance myography. Muscle Nerve. 2010; 42:915–21. [PubMed: 21104866]

Rutkove SB, Zhang H, Schoenfeld DA, Raynor EM, Shefner JM, Cudkowicz ME, et al. Electrical impedance myography to assess outcome in amyotrophic lateral sclerosis clinical trials. Clin Neurophysiol. 2007; 118:2413–8. [PubMed: 17897874]

Shefner JM, Cudkowicz ME, Brown RH Jr. Comparison of incremental with multipoint MUNE methods in transgenic ALS mice. Muscle Nerve. 2002; 25:39–42. [PubMed: 11754183]

Wang L, Ahad M, McEwan A, Li J, Jafarpoor M, Rutkove S. Assessment of alterations in the electrical impedance of muscle after experimental nerve injury via finite element analysis. IEEE Trans Biomed Eng. 2011 Jan 10.

HIGHLIGHTS

- Measurement of surface electrical anisotropy offers a non-invasive, painless means for quantifying neurogenic change in muscle
- Substantial anisotropy alterations in the gastrocnemius muscle of ALS rats were identified with disease progression.
- This change was mainly due to a reduction in longitudinal impedance values, which correlated with age and motor unit number estimates.

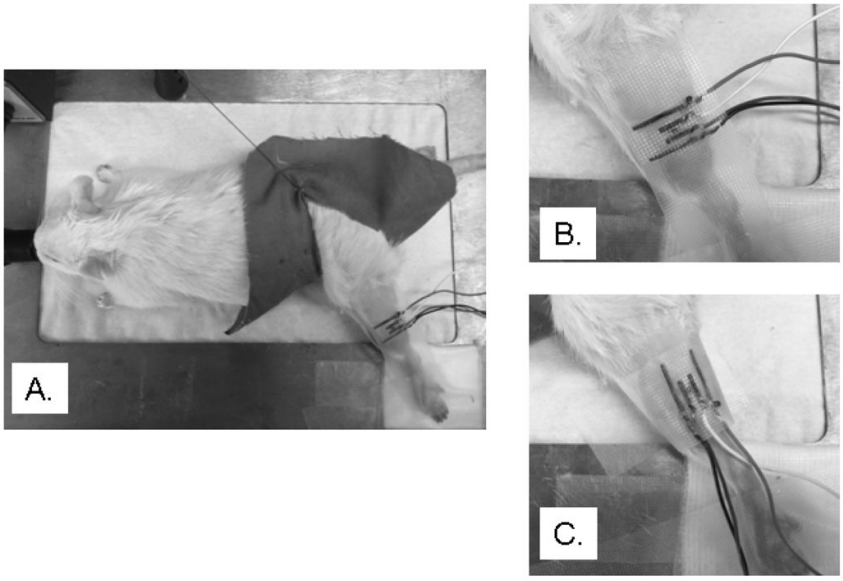

Figure 1.
The experimental setup of the whole animal is presented in the left plot (a). The center (b) and the right (c) plots show the longitudinal (0°) and transverse (90°) electrode positions and the electrodes were marked in dark to be easily seen.

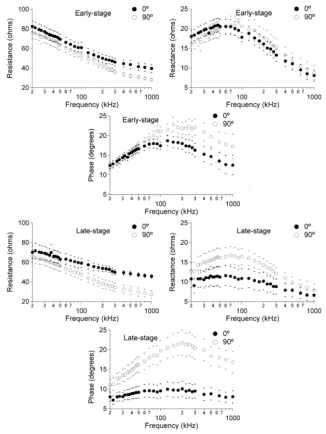

Figure 2.

A comparison of early-stage multi-frequency data (top row) and late-stage data (bottom row) for the 8 animals at 0° (closed circles) and 90° (open circles), each curve confined by its standard error. Note the marked reduction in 0 degree reactance and phase across the frequency spectrum in the late-stage animals.

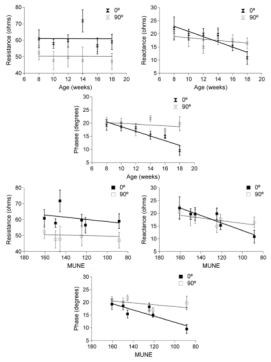

Figure 3.

A comparison of 100 kHz EIM data for 0° and 90° for all three measures across the entire time period. The top row presents the correlation with age and the bottom row shows the correlation with MUNE. To be consistent with age, the horizontal axes of the bottom row are in reverse order. Note the prominent reductions in longitudinal reactance and phase and virtually static resistance data as correlated to age and MUNE.

TABLE 1

Summary of statistical analyses to the impedance measures at 5 frequencies.

		50 kHz	100 kHz	200 kHz	300 kHz	500 kHz
R at 0° (Ω)	Early, Late	69.4 ± 5.65,63.0 ± 6.65	60.9 ± 5.06, 59.0 ± 4.66	50.0 ± 3.93, 53.7 ± 3.24	46.1 ± 3.87, 49.9 ± 2.81	43.5 ± 4.05, 48.4 ± 2.19
	p Value	0.574	0.721	0.234	0.328	0.130
R at 90° (Ω)	Early, Late	64.2 ± 5.36, 55.9 ± 5.14	52.4 ± 4.25, 47.1 ± 4.90	43.0 ± 3.03, 38.1 ± 4.68	36.3 ± 1.87, 34.5 ± 4.22	32.2 ± 1.58, 31.2 ± 4.14
	p Value	0.574	0.574	0.645	1.000	1.000
X at 0° (Ω)	Early, Late	20.5 ± 1.73, 11.2 ± 2.54	17.8 ± 1.17, 10.9 ± 2.48	16.1 ± 1.69, 10.2 ± 2.21	13.3 ± 1.54, 8.8 ± 1.92	11.1 ± 1.55, 7.9 ± 1.66
	p Value	**0.021**	**0.038**	0.161	0.161	0.234
X at 90° (Ω)	Early, Late	20.3 ± 2.16, 16.1 ± 2.31	20.5 ± 2.41, 16.4 ± 2.08	17.7 ± 2.25, 14.3 ± 1.60	15.2 ± 2.18, 12.1 ± 1.42	11.9 ± 1.93, 9.9 ± 1.50
	p Value	0.279	0.195	0.382	0.505	0.505
θ at 0°(°)	Early, Late	16.6 ± 1.03, 9.2 ± 1.49	17.4 ± 0.88, 9.5 ± 1.78	18.0 ± 1.53, 10.1 ± 1.86	16.3 ± 1.72, 9.5 ± 1.76	14.7 ± 2.01, 8.8 ± 1.53
	p Value	**0.001**	**0.001**	**0.005**	**0.021**	**0.050**
θ at 90° (°)	Early, Late	17.4 ± 0.87, 16.1 ± 1.95	21.1 ± 1.18, 19.8 ± 2.66	21.8 ± 1.53, 21.8 ± 3.15	22.1 ± 2.05, 20.4 ± 2.85	19.7 ± 2.41, 18.3 ± 2.36
	p Value	0.161	0.234	0.645	0.382	0.721

p values < 0.05 are in bold. R, resistance; X, reactance; θ, phase.

TABLE 2

Summary of statistical analyses to the anisotropy differences (AD) at 5 frequencies.

		50 kHz	100 kHz	200 kHz	300 kHz	500 kHz
AD for R (Ω)	Early, Late	−5.2 ± 3.69, −7.1 ± 5.93	−8.5 ± 2.58, −11.9 ± 5.74	−7.0 ± 2.89, −15.6 ± 5.52	−9.8 ± 3.32, −15.4 ± 5.42	−11.4 ± 3.74, −17.2 ± 5.09
	p Value	0.878	0.574	0.161	0.574	0.442
AD for X (Ω)	Early, Late	−0.2 ± 1.69, 4.9 ± 1.65	1.1 ± 1.86, 5.6 ± 1.47	1.6 ± 1.54, 4.1 ± 1.20	2.0 ± 1.65, 3.3 ± 1.20	0.8 ± 1.60, 2.0 ± 1.41
	p Value	0.065	**0.050**	0.279	0.442	0.505
AD for θ (°)	Early, Late	0.8 ± 0.93, 7.0 ± 1.56	1.8 ± 1.58, 10.2 ± 2.13	3.9 ± 1.48, 11.7 ± 2.56	5.8 ± 2.02, 10.9 ± 2.21	5.0 ± 2.20, 9.6 ± 1.75
	p Value	**0.015**	**0.028**	**0.038**	0.195	0.279

p values < 0.05 are in bold. R, resistance; X, reactance; θ, phase.

TABLE 3

Summary of the correlation coefficient of the EIM data with age and MUNE.

	Age		MUNE	
	ρ	P value	*ρ*	P value
R at 0° (Ω)	0.31	0.544	0.43	0.397
R at 90° (Ω)	0.26	0.623	0.20	0.704
X at 0° (Ω)	0.83	**0.042**	0.77	0.072
X at 90° (Ω)	0.54	0.266	0.77	0.072
θ at 0° (°)	0.92	**0.010**	0.94	**0.005**
θ at 90° (°)	0.31	0.544	0.60	0.208

p values < 0.05 are in bold. R, resistance; X, reactance; θ, phase.